

Macrofaunal burrowing Enhance Deep-sea Carbonate Lithification on the Southwest Indian Ridge

Hengchao Xu, Xiaotong Peng*, Shun Chen, Jiwei Li, Shamik Dasgupta, Kaiwen Ta, Mengran Du

5 Deep-sea Science Division, Institute of Deep-Sea Science and Engineering, Chinese Academy of Science, Sanya 572000, China

Correspondence to: Xiaotong Peng (xtpeng@idsse.ac.cn)

Abstract. Deep-sea carbonates represent an important type of sedimentary rock due to their effect on the composition of upper oceanic crust and their contribution to deep-sea geochemical cycles. However, roles of deep-sea macrofauna in carbonate lithification remain poorly understood. A large lithified carbonate area, characterized by thriving benthic faunas and tremendous amounts of burrows, was discovered in 2008, blanketed on the seafloor of ultraslow spreading Southwest Indian Ridge (SWIR). Benthic inhabitants including echinoids, polychaetes, gastropods, as well as crustaceans, are abundant in carbonates. The burrowing features within these carbonate rocks, and factors that may influence deep-sea carbonate lithification, were reported. We suggest that burrowing in these carbonate rocks enhance deep-sea carbonate lithification. We propose that active bioturbation may trigger the dissolution of the original calcite and thus accelerate deep-sea carbonate lithification on mid-ocean ridges. Macrofaunal burrowing provides a novel driving force for deep-sea carbonate lithification at the seafloor, illuminating the geological and biological importance of deep-sea carbonate rocks on global mid-ocean ridges.

1 Introduction

Carbonate rocks and sediments of various types have been discovered on mid-ocean ridges through dredging or drilling (Thompson et al., 1968; De et al., 1985; Cooke et al., 2004). These carbonates, which are important elements of the upper oceanic crust, cover approximately half of the area of the entire ocean floor. As such, they may influence the composition of oceanic crust and alter the geochemical balance between the total amounts of calcium, magnesium, and carbon in oceanic waters (Holligan and Robertson, 1996; Rae et al., 2011; Yu et al., 2014; Anderson et al., 1976).

Most carbonates in the deep sea are biogenic in origin and may involve diagenetic products that originate from calcareous biogenic debris. Loss of porosity with increasing age and burial depth is associated with the transformation of deep-sea calcareous ooze to chalk, and subsequently to limestone (Flügel, 2004). Nevertheless, processes involved in the formation of deep-sea carbonate rocks remain controversial. It has commonly been assumed that deep-sea carbonate lithification is driven by various processes, including gravitational compaction, pressure dissolution, and reprecipitation that takes place during burial (Croizé et al., 2013). Local dissolution and reprecipitation of biogenic calcite or aragonite from

foraminifera, nanofossils, and pteropod oozes may serve to transform the original sediments to chalk or limestone (Schlanger and Douglas, 1974). These explanations, however, cannot completely explain the facts that (i) the degree of burial is commonly inconsistent with the known burial depth and paleontological age (Schmoker and Halley, 1982), and (ii) lithified carbonate rocks found on the seafloor commonly show no evidence of burial (Thompson et al., 1968). Lithification of deep-sea carbonates has also been associated with the breakdown of oceanic basalts or prolonged exposure to the chemical gradients at the sediment-water interface (Pimm et al., 1971; Bernoulli et al., 1978). However, the processes responsible for such seafloor lithification remain debatable.

Benthic fauna drilling into the substrate play a critical role in sediment evolution, because of enhanced interactions between sediments, interstitial water and overlying water, by changing the geochemical gradients in the sediment, restructuring bacterial communities, and influencing the physical characteristics of the sediments (Lohrer et al., 2004; Meysman et al., 2006; Barsanti et al., 2011; Lalonde et al., 2010). Although burrowing has already been recognized as a factor that may influence CaCO_3 sediment profiles (Emerson and Bender, 1981; Aller, 1982; Emerson et al., 1985; Green et al., 1992), and may promote carbonate dissolution in coastal sediments (Gerino et al., 1998), little is known about the lithification effects of semi-lithified and lithified carbonate rocks in deep sea settings.

Non-burial carbonate samples were collected in 2008 near a newly discovered hydrothermal vent on Southwest Indian Ridge (SWIR) during the DY115-20 cruise of R/V Dayang Yihao, which was conducted by the China Ocean Mineral Resource R&D Association (COMRA) (Fig. 1). These carbonate rocks, which were associated with a thriving benthic biota, are characterized by numerous macrofaunal burrows. In this research, we attempted to explore the unique non-burial carbonate lithification in the deep-sea and to highlight the interactions that take place between bioturbation and lithification on the mid-ocean ridge.

2. Geological Setting

The Southwest Indian Ridge (SWIR), which is the major boundary between the Antarctic Plate and the African Plate, and characterized by its ultraslow and oblique expansion, is one of the slowest-spreading ridges (1.4-1.6 cm/yr) in the global ocean ridge system (Dick et al., 2003). Three main ridge sections of eastern part of the SWIR are divided by the Gallieni Transform Fault (GTF) and the Melville Transform Fault (MTF) (Cannat et al., 1999). In 2008, a large lithified carbonate area, approximately 15 km long and 150 km wide at 2000 to 2500 m water depths, was found on segment 26 of the SWIR, near a newly discovered hydrothermal field (Fig. 1). It has been widely reported that primary productivity increased substantially at the Indian Ocean during the Latest Miocene–Early Pliocene (Arumugm et al., 2014; Gupta et al., 2004; Rai and Singh, 2001; Singh et al., 2012). This phenomenon known as “biogenic bloom” promoted significantly high quantities of carbonate deposits at the seafloor between 9 to 3.5Ma (Gupta et al., 2004; Dickens and Owen, 1999).

3. Material and Methods

3.1 Sampling

The deep-sea carbonate samples were collected in 2008 by TV-grabs bucket operated from the R/V Da Yang Yi Hao. The survey sites covered an area of approximately 15 km long and 150 km wide. When carbonate samples were spread on the deck, benthic organisms were usually evident among the fractured rocks. Samples were subsampled after recovery, and then stored at -20°C in plastic bags for mineralogical and geochemical analysis. Subsamples for molecular phylogenetic analysis were kept in dry ice frozen and transported to the laboratory.

3.2 Computerized X-ray tomography (CT)

Quantitative measurement of the significance of biological influence is difficult because the physico-chemical properties around burrow walls are dynamic. Computerized X-ray tomography is a non-destructive method that has been used to measure various rock properties (e.g., bulk density, porosity, macropore size), by determining the numerical value of the X-ray attenuation coefficient. For relatively homogeneous marine sediments, this coefficient is expressed as Hounsfield units (HU), which is correlated with sample density (Michaud et al., 2003). In this study, computerized X-ray tomography measurements were performed using a GE Light Speed VCT instrument located in the Shanghai 10th People Hospital, Tongji University. CT images were computerized by reconstruction of the distribution function of the linear attenuation coefficient, each with a 64-slice system with 64×0.625 mm detector banks and a z-axis coverage of 40 mm. The slice thickness was 2.5 mm and the accuracy of distance measurements in the x and y-planes was 0.2 mm. The instrument operated at 140 kV, with a 10 mA current, and 1.5 s exposure.

CT images were further characterized by *Image J*, which was a public domain Java-based image processing program. Gray values, which correlated with the attenuation values and HU, were extracted to make a comparing description of the density changes of the carbonate sample. 40 CT images were selected, and each gray value inverted using $\text{min} = 0$ and $\text{max} = 255$, regardless of the data values; that was, the theoretical integrated density value without the carbonate sample will be close to zero. The calibration function was used to calibrate whole images to a set of density standards before extracting. After all images selected were calibrated, the integrated density of the rock around the burrows could be calculated from the gray values. For this study, the gray values of the 10 pixels (approximately 0.3 cm, compared to the diameters of burrows are approximately 0.9 cm) around the burrow holes were measured. Additionally, randomly selected areas away from the burrows were selected as controls. Function of “polyfit” in MATLAB was used to interpret the difference between two data sets with 95% confidence bounds.

3.3 X-ray diffraction (XRD)

Small pieces of the samples, which were freeze-dried under vacuum conditions to avoid oxidation during drying, were thoroughly ground using a pestle and mortar to produce a fine-grained, uniform powder. These powders were analysed using

a D/max2550VB3+/PC X-ray diffractometer (Rigaku Corporation) at 40 kV and 30 mA, which is housed at the State Key Laboratory of Marine Geology at Tongji University.

3.4 Scanning electron microscope (SEM)

5 Small fragments of the dried samples were fixed onto aluminum stubs with two-way adherent tabs, and allowed to dry overnight. They were sputter coated with gold for 2-3 minutes before being examined on a Philips XL-30 scanning electron microscope equipped with an accelerating voltage of 15kV at the State Key Laboratory of Marine Geology, Tongji University. The elemental composition of selected spots was determined by energy dispersive X-ray (EDX) analysis on the SEM with an accelerating voltage of 20 kV.

3.5 Element and isotope analysis

10 After fusion of 0.1 g of sample material with 3.6 g of dilithium tetraborate at 1050 °C for ca. 16 min, major elements were measured using X-ray fluorescence Shimadzu XRF-1800 spectrometer at 40 kV and 95 mA that is located at Shanghai University. The trace element and rare earth element (REE) compositions of the samples were determined by inductively coupled plasma-mass spectrometry (ICP-MS) using a Thermo VG-X7 mass spectrometer at the State Key Laboratory of Marine Geology, Tongji University. Samples for these analyses were dissolved using a solution of HNO₃ + HF on a hot plate.
15 The eluted sample was then diluted with 2% HNO₃. The analytical precision and accuracy, monitored by geostandard GSD9 and sample duplicates, were better than 5%.

Stable oxygen and carbon isotope ratios of bulk samples were measured using a Finnigan MAT252 isotope ratio mass spectrometer equipped with a Kiel III carbonate device at the State Key Laboratory of Marine Geology, Tongji University. Bulk samples were oven-dried at 60°C. Analytical precision was monitored using the Chinese national carbonate standard,
20 GBW04405. Conversion of measurements to the Vienna Peedee Belemnite (PDB) scale was performed using NBS-19 and NBS-18.

4. Results

4.1 Macroscopic observations

The carbonate rocks retrieved from the SWIR were characterized by complex honeycombed structures, with Mn- and
25 Fe-oxides commonly encrusting the surface and inner surface of carbonate rocks (Fig. 2). Benthic inhabitants, including echinoids, polychaetes, gastropods, and crustaceans, which are usually recognized as successful burrowing classes in marine sediments (Kristensen and Kostka, 2013), were abundant in hand specimens (Fig. 2c, d). Burrows drilled by benthic fauna showed from CT scanning images are in straight, branched, or J- and U-shaped, with density up to 12 per dm² (Fig. S1). Burrows commonly penetrate 6 to 10 cm into the rock with several millimetres to 2 cm in diameter. The area that surrounds

the hole is usually brighter than that away from the burrow, which may indicate a different degree of lithification (Fig. 3a, 4a). Burrows can be classified in three categories. Burrows with living organisms can be categorized explicitly as fresh burrows (Fig. 2c, d). The second type is considered to be the vacant burrows which are filled by gray excrements (Fig. 2b). Thin black Mn- and Fe-oxide precipitates commonly encrust the surface of carbonate and the inner surface of empty burrows (Fig. 2a, c, d) and thus are classified as the third type of burrow. It has been suggested that Mn- and Fe-oxide precipitates grow at a very slow rate of 1-10mm/Ma. Coating of black Mn- and Fe-oxide precipitates on the surface of the burrows indicate that they may form much earlier than other burrows. Thus, the influence of bioturbation in this area is most likely a continuous process during the early lithification and could play a significant role in both geological and biological processes.

4.2 Enhanced lithification around burrow

Computerized X-ray tomography (CT) was used for better characterization of local changes of density in the carbonate rocks, which would reflect their degree of lithification. A darker colour in the tomographic cross-section image of the sample represents lower attenuation and thus lower density and higher porosity. The most apparent feature of the CT image is localized enhancement of density around the burrow (Fig. 3, 4). The shapes of the area with higher density around the holes are triangular, quadrangular, hexagonal, round or irregular (Fig. 3b, c). Integrated density profiles extracted from the tomographic cross-section images make the contrast of density change around the burrow more clear (Fig. 3d). 3D reconstruction of the sample by CT exhibits that the enhancement of density is visible around the burrow, which is consistent with the enhancement of brightness around the burrow as shown in hand specimen (Fig. 4). Statistical analysis of density of 113 burrows (Fig. 5) provides robust evidence for density enhancement around the burrows, illuminating the significant influence of bioturbation in lithification. In addition, the results of CT also show that density is generally higher at the bottom than at the top of the carbonate rocks (Fig. 4c).

4.3 Mineralogy

Based on XRD and elemental analyses, rock samples consisted almost entirely of calcite and detectable quartz, halite which are typical for deep-sea chalk defined as soft, pure, earthy, fine-textured, usually white to light gray or buff limestone of marine origin, consisting almost wholly (90-99%) of calcite, formed mainly by accumulation of calcareous tests of floating micro-organisms (chiefly foraminifers) and of comminute remains of calcareous algae (such as coccoliths and rhabdoliths) set in a structureless matrix of very finely crystalline calcite (Wolfe, 1968; Flügel, 2004). Thin section and scanning electron photomicrographs show that biogenic components, mainly planktonic foraminifera (*Globigerina bulloides*) and coccolithophorid (*Coccolithus pelagicus*) dominate (Fig. 6). The presence of *Globigerina bulloides* indicates that the lithification history of carbonate rocks is less than 5 Ma (Pliocene-Recent) old. Therefore, carbonate deposit on the SWIR could be bioclastic deposition from the productivity related events 'biogenic bloom' to large part of Indian Ocean during middle Miocene to the early Pliocene (Singh et al., 2012; Rai and Singh, 2001; Gupta et al., 2004; Arumugm et al., 2014).

Although it was difficult to separate and quantify the small tests from the very fine matrix, the carbonates exhibited a relatively high test to matrix ratio that is representative of deep-sea chalk (Fig. 6a). Original skeletal grains were held together by cement. Body chambers in the foraminiferal tests, for instance, were partially filled by calcite cements (Fig. 6b, c). It was common to observe the accretionary overgrowth of calcite around the foraminifera test from SEM images (Fig. 6c).
5 Dissolution of the coccolith plates is evident both on the surface of the thin black Mn- and Fe-oxide precipitates and in the interior of carbonate rocks (Fig. 6e). The gray excrements filling in the burrow primarily consisted of plates of coccolithophorids (*Calcidiscus leptoporus*, *Emiliana huxleyi* and *Gephurocapsa oceanica*). Smooth surfaces of the coccoliths in gray excrements revealed that dissolution commonly occurs influenced by bioleaching of benthic fauna (Fig. 6f).

10 4.4 Geochemistry and isotope analysis

Three types of samples (chalk, gray excrements and thin black Mn- and Fe-oxide precipitates) exhibited similar elemental concentration patterns for high CaO content, reflecting the strong dilution effect of biogenic calcium (Table S1). One of the main characteristics of major and rare elements is the highly variable Sr concentrations in different types of the sample. The storage of Sr on seafloor is mainly caused by substitution of Ca in calcium carbonate while diagenetic
15 recrystallization results in the decrease of Sr from the sediment (Plank and Langmuir, 1998; Qing and Veizer, 1994). The lower Sr/Ca ratio in chalk compared to the gray excrements could also be a response to the lithification of carbonate (Fig. 7). Although biogenic calcium diluted the detrital REE fraction, it made little direct contribution to bulk REE concentrations (Xiong et al., 2012). REE patterns of the three types of sample did not exhibit any hydrothermal anomalies, e.g. positive Eu anomaly, but inherit the characteristics of sea water by enrichment of HREE compared with LREE and negative Ce anomaly
20 (except the Mn- and Fe-oxide) (Fig. 8). The influence of nearby hydrothermal system and other detrital input to the studied carbonate area should be negligible during the lithification history.

The $\delta^{13}\text{C}_{\text{PDB}}$ values of 46 bulk samples were -0.37 to 1.86‰ which are typical for biogenic carbonates (e.g. Cook and Egbert 1979). These samples have a relatively narrow $\delta^{18}\text{O}_{\text{PDB}}$ range of 1.35 to 3.79‰. Positive correlation of $\delta^{13}\text{C}_{\text{PDB}}$ and $\delta^{18}\text{O}_{\text{PDB}}$ values of chalk and gray excrements ($r = 0.91$) reveals minor environmental influence on early lithification (Fig. 9)
25 and bioturbation should be a critical factor during the lithification. There is an evident depletion of carbon and oxygen isotopic values of gray excrements compared to chalks (Fig. 9). Carbon isotope signatures of carbonates near burrow with higher density were relatively high compared to undisturbed areas (Table 1).

5. Discussion

5.1 Bioturbation in carbonate rock on SWIR

The dimensions of burrows can be estimated from tomographic cross-section of the samples. Burrows were generally few millimetres to 2 cm in diameter, commonly penetrating 6 to 10 cm into the rocks and ultimately reaching a density of up to 12 per dm². If burrows in straight, branched, or J- and U-shaped (Fig. 2e) are simplified to a cylinder with the diameter of 1 cm and height of 6 cm, which are the median value of the burrows, estimated volume of the simplified cylinder would be helpful to reckon the extent of substratum reconstruction by bioturbation. In this model, 1 dm² surface area which can harbor 12 burrows on the surface may reach to 0.226 dm³ burrow space. Eventually, we can deduce that carbonate substratum is reconstructed by bioturbation to a great extent.

Benthic fauna maintain burrows for certain purposes of gaseous exchange, food transport, gamete transport, transport of environmental stimuli, and removal of metabolites (Kristensen and Kostka, 2013). Polychaetes, the most successful burrow class for example (Díaz-Castañeda and Reish, 2009), were abundant and conventionally produced J- or U- shaped burrow extended as long as several decimetres in hand specimens (Fig. 2 c, e). Relic burrows allow sea water to directly penetrate into carbonate rocks, which is beneficial to the precipitation of black Mn- and Fe-oxide precipitates on the inner surface of burrow (Fig. 2a, c). The genetic models for Mn- and Fe-oxide precipitates has been attributed to the minerals precipitated out of the cold ambient seawater onto the rock surface with the aid of biogenic activity (Hein and Koschinsky, 2014). Burrowing benthic fauna excrete mucus to garden their burrow holes by incorporating organic matter into the walls (Dworschak et al., 2006; Koller et al., 2006). The mucus layer may act as favourable site for the accumulation of metallic ions through organo-metallic complexation or chelation at suitable Eh, pH and redox conditions (Lalonde et al., 2010; Banerjee, 2000). Thus, along with carbonate reworking and bio-mixing during frequent construction and maintenance of burrow, mineralogical and geochemical parameters, are also assumed to oscillate around the burrow.

In addition to the burrowing activity, benthic fauna ingest and excrete the substrate which usually serve the burrows as traps for fecal pellets (Fig. 2b) (Hydes, 1982; Aller and Aller, 1986). Although benthic fauna ingest organically enriched particles, thus removing the organic matter, bulk sample is often still enriched in residual fecal material (Dauwe et al., 1998). Regardless, organic matter influenced by bioturbation and delivered as biodeposits in surface sediments, and vice versa, may therefore create a dynamic and heterogeneous chemical, physical, and biological micro-environment in the deep-sea carbonate zones. Eventually, a microenvironment friendly for heterotrophic microorganism may be formed in the carbonate due to redistribution of organic particles. The biodiversity of the prokaryotic communities within the samples examined by Li et al. (2014) inferred that the distribution of Acidobacteria and Bacteroidetes noted in this study might indicate the greater organic carbon availability in the interior carbonates. Alternatively, bacterial metabolites and organic detritus are considered to be the major sources of food for benthic fauna in deep-sea environment, which is limited by availability of organic matter (Raghukumar et al., 2001). Thus, a balanced ecological sustainability is established by the carbonate deposits and continuous biological processes, which may largely influence the lithification history of the carbonates.

5. 2 Roles of bioturbation in lithification of carbonate rocks on the SWIR

Abundant macrofaunal burrows, as well as benthic fauna (e.g. polychaete worm, Fig. 2c) present on a cross section of carbonate rocks and enhancement of density around burrows commonly observed from CT images (Fig. 3, 4), provided robust evidence for the significant role of bioturbation in present lithified deep-sea carbonates. The lithification of carbonate is confirmed by the dissolution of coccolith plates observed by SEM (Fig. 6) and elemental composition change between different portions of the carbonate (Fig. 7). Water depth of studied carbonate area on SWIR varies approximately from 2000 to 2500 meters (Fig. 1), which is above the calcite saturation horizon (Broecker et al., 1982). In this range of water depth, the key point of carbonate lithification is how original tests or plates are dissolved under saturation condition. Although less stable CaCO_3 phase (e.g., biogenic, high-Mg calcites) may dissolve above the calcite saturation horizon (Jahnke and Jahnke, 2004), they are not likely to happen here, since our samples are low-Mg calcites. As a general rule, compaction takes place with gradual increase of overburden pressure, resulting in loss of porosity through mechanical and chemical compaction in moderate-deep burial stage. However, present carbonate samples show they have never been buried. Their lithification therefore may be different from other deep sea carbonates. Elements and isotope results reveal minor external impact on the early lithification. The construction and ventilation of burrows can fundamentally alter biogeochemical processes and produce lateral heterogeneity intensifying the redistribution of pore water fluids. Moreover, the ecological niches for microbial life are also formed by bioturbation (Ghirardelli, 2002; Koretsky et al., 2013). Thus, the simultaneous activities of both thriving benthic fauna and lithification of carbonate, are potentially connected.

The organic matter is possibly significantly low in the deep-sea sediment. However, the distribution and diversity of the prokaryotic communities inhabiting carbonate samples imply the greater organic carbon availability in the interior carbonates compared to the exterior (Li et al., 2014). It is known that polychaetes' mixing sediment particles is an important driving force behind chemical reaction and transport of organic matter in marine sediments (Levinton et al., 1995). Benthic fauna, including polychaetes, reconstruct the carbonate substratum to a great extent and result in a fundamental alteration of sedimentary environment. Aerobic respiration of bioturbated organic particles like mucus would positively contribute to the aerobic respiration of bioturbated organic particles by heterotrophic (micro)organisms (Lohrer et al., 2004), whose reaction product CO_2 may be responsible for lowering the pH of porewater around the burrow relative to the inner carbonate sediment, which may drive the dissolution of original calcite in microenvironment (Fig. 10) (Emerson and Bender, 1981; Aller, 1982; Kristensen, 2000). Isotopic composition in gray excrements is lighter compared to the chalks (Fig. 9; table 1). It is assumed that faecal pellets may strongly depleted in ^{13}C in isotopic mass balance with the ^{13}C enrichment of the organism (Damste et al., 2002). That means bioturbated organic particles like mucus will inherit enriched ^{13}C , which is the major carbon source for microbial metabolic reaction. The local elevated concentration of dissolved CO_2 in pore water would trigger the dissolution of the original CaCO_3 phases, which is consistent with the results of SEM observation. For instance, body chambers in the foraminiferal tests are partially filled by calcite cements (Fig. 6c), which is believed to be derived internally through solution transfer (Durney, 1972).

In addition, relic burrows make sea water directly penetrate into carbonate rocks and lead to the precipitation of black Mn- and Fe-oxide precipitates in the inner surface of the burrow. Microbial oxidation of Fe^{2+} and Mn^{2+} in these sites would also greatly accelerate the dissolution of CaCO_3 fossils (Emerson and Bender, 1981; Aller and Rude, 1988). Furthermore, thin Mn- and Fe-oxide precipitates may prevent the rapid ion exchange between bottom water and porewater within carbonate rocks. Ca^{2+} and CO_3^{2-} , the products of CaCO_3 dissolution, prefer to diffuse to the interior of carbonate rocks, and lead to the reprecipitation of calcites as cements with higher $\delta^{13}\text{C}_{\text{PDB}}$ in carbonate rocks (Fig. 10).

6. Conclusions

A lithified carbonate area characterized by active bioturbation was studied to explore the area's biological and geological interactions. Although the effect of different parameters influenced by bioturbation cannot easily be differentiated in study of natural samples, available evidences show that active bioturbations may trigger the dissolution of original calcite above the saturation horizon, thus enhancing deep-sea carbonate lithification on mid-ocean ridges. The novel mechanism proposed here for non-burial carbonate lithification at the deep-sea seafloor sheds light on the potential interactions between deep-sea biota and sedimentary rocks, and also illuminate the geological and biological importance of deep-sea carbonate rocks on mid-ocean ridges.

15 Acknowledgments

Special thanks go to all the participants of the cruise of R/V DayangYihao conducted by China Ocean Mineral Resource R&D Association (COMRA) in 2008. The authors also would like to acknowledge Dr. Sui Wan at Tongji University for his help with the calcareous fossil analysis. Financial support for this research came from "Strategic Priority Research Program" of the Chinese Academy of Science (Grant No. XDB06020201), "National Key Basic Research Program of China" (2015CB755905), "Natural Science Foundation of Hainan Province, China" (20164175). We are indebted to Prof. Brian Jones at University of Alberta for his valuable suggestions on the manuscript. We are greatly indebted to two anonymous journal reviewers, and the journal associate editor, Caroline Slomp for their critical comments on an earlier version of this manuscript.

References

25 Aller, J. Y., and Aller, R. C.: Evidence for localized enhancement of biological associated with tube and burrow structures in deep-sea sediments at the HEEBLE site, western North Atlantic, Deep Sea Research Part a. *Oceanographic Research Papers*, 33, 755-790, 1986.

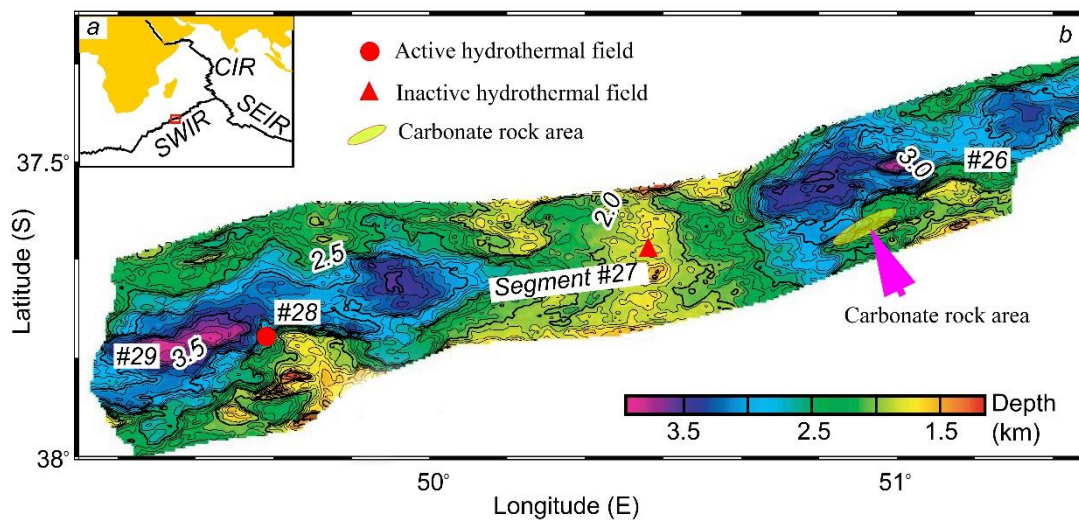
- Aller, R. C.: Carbonate dissolution in nearshore terrigenous muds: the role of physical and biological reworking, *The Journal of Geology*, 90, 79-95, 1982.
- Aller, R. C., and Rude, P. D.: Complete oxidation of solid phase sulfides by manganese and bacteria in anoxic marine sediments, *Geochimica et Cosmochimica Acta*, 52, 751-765, 1988.
- 5 Anderson, T., Donnelly, T., Drever, J., Eslinger, E., Gieskes, J., Kastner, M., Lawrence, J., and Perry, E.: Geochemistry and diagenesis of deep-sea sediments from Leg 35 of the Deep Sea Drilling Project, *Nature*, 261, 473-476, <https://doi.org/10.1038/261473a0>, 1976.
- Arumugm, Y., Gupta, A. K., and Panigrahi, M. K.: Species diversity variations in Neogene deep-sea benthic foraminifera at ODP Hole 730A, western Arabian Sea, *Journal of Earth System Science*, 123, 1671-1680, [https://doi.org/10.1007/s12040-](https://doi.org/10.1007/s12040-10)
- 10 014-0495-z, 2014.
- Banerjee: A documentation on burrows in hard substrates of ferromanganese crusts and associated soft sediments from the Central Indian Ocean, *Current Science*, 79, 517-521, 2000.
- Barsanti, M., Delbono, I., Schirone, A., Langone, L., Miserocchi, S., Salvi, S., and Delfanti, R.: Sediment reworking rates in deep sediments of the Mediterranean Sea, *Science of The Total Environment*, 409, 2959-2970, <http://doi.org/10.1016/j.scitotenv.2011.04.025>, 2011.
- 15 Bernoulli, D., Garrison, R., and McKenzie, J.: Petrology, isotope geochemistry, and origin of dolomite and limestone associated with basaltic breccia, Hole 373A, Tyrrhenian Basin, in: *Initial Reports of the Deep Sea Drilling Project*, edited by: KJ Hsü, and Montadert, L., 1, U. S. Government Printing Office, Washington 541-558, 1978.
- Broecker, W. S., Peng, T.-H., and Beng, Z.: *Tracers in the Sea*, Lamont-Doherty Geological Observatory, Columbia University, New York, 1982.
- 20 Cannat, M., Rommevaux-Jestin, C., Sauter, D., Deplus, C., and Mendel, V.: Formation of the axial relief at the very slow spreading Southwest Indian Ridge (49 to 69 E), *Journal of Geophysical Research: Solid Earth* (1978–2012), 104, 2825-2843, <https://doi.org/10.1029/1999JB900195>, 1999.
- Cook H. E., Egbert R.M.: Diagenesis of Deep-Sea Carbonates. in: Larsen G, Chilingar GV, eds. *Developments in Sedimentology*, Elsevier. 213-288, 1979.
- 25 Cooke, P. J., Nelson, C. S., Crundwell, M. P., Field, B., Elkington, E. S., and Stone, H.: Textural variations in Neogene pelagic carbonate ooze at DSDP Site 593, southern Tasman Sea, and their paleoceanographic implications, *New Zealand Journal of Geology and Geophysics*, 47, 787-807, 2004.
- Croizé, D., Renard, F., and Gratier, J.-P.: Compaction and Porosity Reduction in Carbonates: A Review of Observations, Theory, and Experiments, *Advances in Geophysics*, 54, 181-238, <http://doi.org/10.1016/B978-0-12-380940-7.00003-2>, 2013.
- 30 Díaz-Castañeda, V., and Reish, D. J.: Polychaetes in Environmental Studies, in: *Annelids in Modern Biology*, John Wiley & Sons, Inc., 203-227, 2009.

- Damste, J. S. S., Breteler, W. C. M. K., Grice, K., Van Rooy, J., and Schmid, M.: Stable carbon isotope fractionation in the marine copepod *Temora longicornis* : Unexpectedly low $\delta^{13}\text{C}$ value of faecal pellets, *Marine Ecology Progress Series*, 240, 195-204, <https://doi.org/10.3354/meps240195>, 2002.
- Dauwe, B., Herman, P. M. J., and Heip, C. H. R.: Community structure and bioturbation potential of macrofauna at four
5 North Sea stations with contrasting food supply, *Marine Ecology Progress Series*, 173, 67-83, <https://doi.org/10.3354/meps173067>, 1998.
- De, R., Rao, C. N., and Kaul, I. K.: Implications of diagenesis for the TL dating of the oceanic carbonate sediments in the Northern Indian ocean, *Nuclear Tracks and Radiation Measurements*, 10, 185-192, 1985.
- Dick, H. J., Lin, J., and Schouten, H.: An ultraslow-spreading class of ocean ridge, *Nature*, 426, 405-412, DOI:
10 10.1038/nature02128, 2003.
- Dickens, G. R., and Owen, R. M.: The Latest Miocene–Early Pliocene biogenic bloom: a revised Indian Ocean perspective, *Marine Geology*, 161, 75-91, [http://doi.org/10.1016/S0025-3227\(99\)00057-2](http://doi.org/10.1016/S0025-3227(99)00057-2), 1999.
- Dworschak, P. C., Koller, H., and Abed-Navandi, D.: Burrow structure, burrowing and feeding behaviour of *Corallianassa longiventris* and *Pestarella tyrrhena* (Crustacea, Thalassinidea, Callianassidae), *Marine Biology*, 148, 1369-1382,
15 <https://doi.org/10.1007/s00227-005-0161-8>, 2006.
- Emerson, S., and Bender, M.: Carbon fluxes at the sediment-water interface of the deep-sea: calcium carbonate preservation, *Journal of Marine Research*, 39, 139-162, 1981.
- Emerson, S., Fischer, K., Reimers, C., and Heggie, D.: Organic carbon dynamics and preservation in deep-sea sediments, *Deep Sea Research Part A. Oceanographic Research Papers*, 32, 1-21, 1985.
- 20 Flügel, E.: Diagenesis, Porosity, and Dolomitization, in: *Microfacies of Carbonate Rocks: Analysis, Interpretation and Application*, Springer Berlin Heidelberg, 267-338, 2004, https://doi.org/10.1007/978-3-662-08726-8_7. Furukawa, Y.: Biogeochemical consequences of macrofauna burrow ventilation, *Geochemical Transactions*, 2, 1-9, <https://doi.org/10.1186/1467-4866-2-83>, 2001.
- Gerino, M., Aller, R. C., Lee, C., Cochran, J. K., Aller, J. Y., Green, M. A., and Hirschberg, D.: Comparison of Different
25 Tracers and Methods Used to Quantify Bioturbation During a Spring Bloom: 234-Thorium, Luminophores and Chlorophylla, *Estuarine, Coastal and Shelf Science*, 46, 531-547, <http://doi.org/10.1006/ecss.1997.0298>, 1998.
- Ghirardelli: Endolithic Microorganisms in Live and Dead Thalli of Coralline Red Algae (Corallinales, Rhodophyta) in the Northern Adriatic Sea, *Acta geológica hispánica*, 37, 53-60, 2002.
- Green, M. A., Aller, R. C., and Aller, J. Y.: Experimental evaluation of the influences of biogenic reworking on carbonate
30 preservation in nearshore sediments, *Marine Geology*, 107, 175-181, 1992.
- Gupta, A. K., Singh, R. K., Joseph, S., and Thomas, E.: Indian Ocean high-productivity event (10–8 Ma): Linked to global cooling or to the initiation of the Indian monsoons?, *Geology*, 32, 753-756, <https://doi.org/10.1130/g20662.1>, 2004.
- Hein, J. R., and Koschinsky, A.: Deep-Ocean Ferromanganese Crusts and Nodules A2 - Holland, Heinrich D, in: *Treatise on Geochemistry (Second Edition)*, edited by: Turekian, K. K., Elsevier, Oxford, 273-291, 2014.

- Holligan, P. M., and Robertson, J. E.: Significance of ocean carbonate budgets for the global carbon cycle, *Global Change Biology*, 2, 85-95, <https://doi.org/10.1111/j.1365-2486.1996.tb00053.x>, 1996.
- Hydes, D. J.: *Animal burrows in deep-sea sediments*, 1982.
- Jahnke, R. A., and Jahnke, D. B.: Calcium carbonate dissolution in deep sea sediments: Reconciling microelectrode, pore water and benthic flux chamber results, *Geochimica et Cosmochimica Acta*, 68, 47-59, [https://doi.org/10.1016/S0016-7037\(03\)00260-6](https://doi.org/10.1016/S0016-7037(03)00260-6), 2004.
- Koller, H., Dworschak, P. C., and Abed-Navandi, D.: Burrows of *Pestarella tyrrhena* (Decapoda: Thalassinidea): hot spots for Nematoda, Foraminifera and bacterial densities, *Journal of the Marine Biological Association of the United Kingdom*, 86, 1113-1122, <https://doi.org/doi:10.1017/S0025315406014093>, 2006.
- 10 Koretsky, C. M., Meile, C., and Van Cappellen, P.: Incorporating Ecological and Biogeochemical Information into Irrigation Models, in: *Interactions Between Macro- and Microorganisms in Marine Sediments*, American Geophysical Union, 341-350, <https://doi.org/10.1029/CE060p0341>, 2013.
- Kristensen, E.: Organic matter diagenesis at the oxic/anoxic interface in coastal marine sediments, with emphasis on the role of burrowing animals, *Hydrobiologia*, 426, 1-24, <https://doi.org/10.1023/a:1003980226194>, 2000.
- 15 Kristensen, E., and Kostka, J. E.: Macrofaunal Burrows and Irrigation in Marine Sediment: Microbiological and Biogeochemical Interactions, in: *Interactions Between Macro- and Microorganisms in Marine Sediments*, American Geophysical Union, 125-157, <https://doi.org/10.1029/CE060p0125>, 2013.
- Lalonde, S. V., Dafoe, L. T., Pemberton, S. G., Gingras, M. K., and Konhauser, K. O.: Investigating the geochemical impact of burrowing animals: Proton and cadmium adsorption onto the mucus lining of Terebellid polychaete worms, *Chemical Geology*, 271, 44-51, <https://doi.org/10.1016/j.chemgeo.2009.12.010>, 2010.
- 20 Levinton, J.S., Martinez, D.E., McCartney, M.M., Judge, M.L.: The effect of water flow on movement, burrowing, and distributions of the gastropod *Ilyanassa obsoleta* in a tidal creek. *Marine. Biology*, 122, 417 – 424, 1995.
- Li, J., Peng, X., Zhou, H., Li, J., Sun, Z., and Chen, S.: Microbial Communities in Semi-consolidated Carbonate Sediments of the Southwest Indian Ridge, *Journal of Microbiology*, 52, 111-119, <https://doi.org/10.1007/s12275-014-3133-1>, 2014.
- 25 Lohrer, A. M., Thrush, S. F., and Gibbs, M. M.: Bioturbators enhance ecosystem function through complex biogeochemical interactions, *Nature*, 431, 1092-1095, DOI: 10.1038/nature03042, 2004.
- Meysman, F. J., Middelburg, J. J., and Heip, C. H.: Bioturbation: a fresh look at Darwin's last idea, *Trends in Ecology & Evolution*, 21, 688-695, <https://doi.org/10.1016/j.tree.2006.08.002>, 2006.
- 30 Michaud, E., Desrosiers, G., Long, B., De Montety, L., Crémer, J.-F., Pelletier, E., Locat, J., Gilbert, F., and Stora, G.: Use of axial tomography to follow temporal changes of benthic communities in an unstable sedimentary environment (Baie des Ha! Ha!, Saguenay Fjord), *Journal of Experimental Marine Biology and Ecology*, 285, 265-282, [https://doi.org/10.1016/S0022-0981\(02\)00532-4](https://doi.org/10.1016/S0022-0981(02)00532-4), 2003.

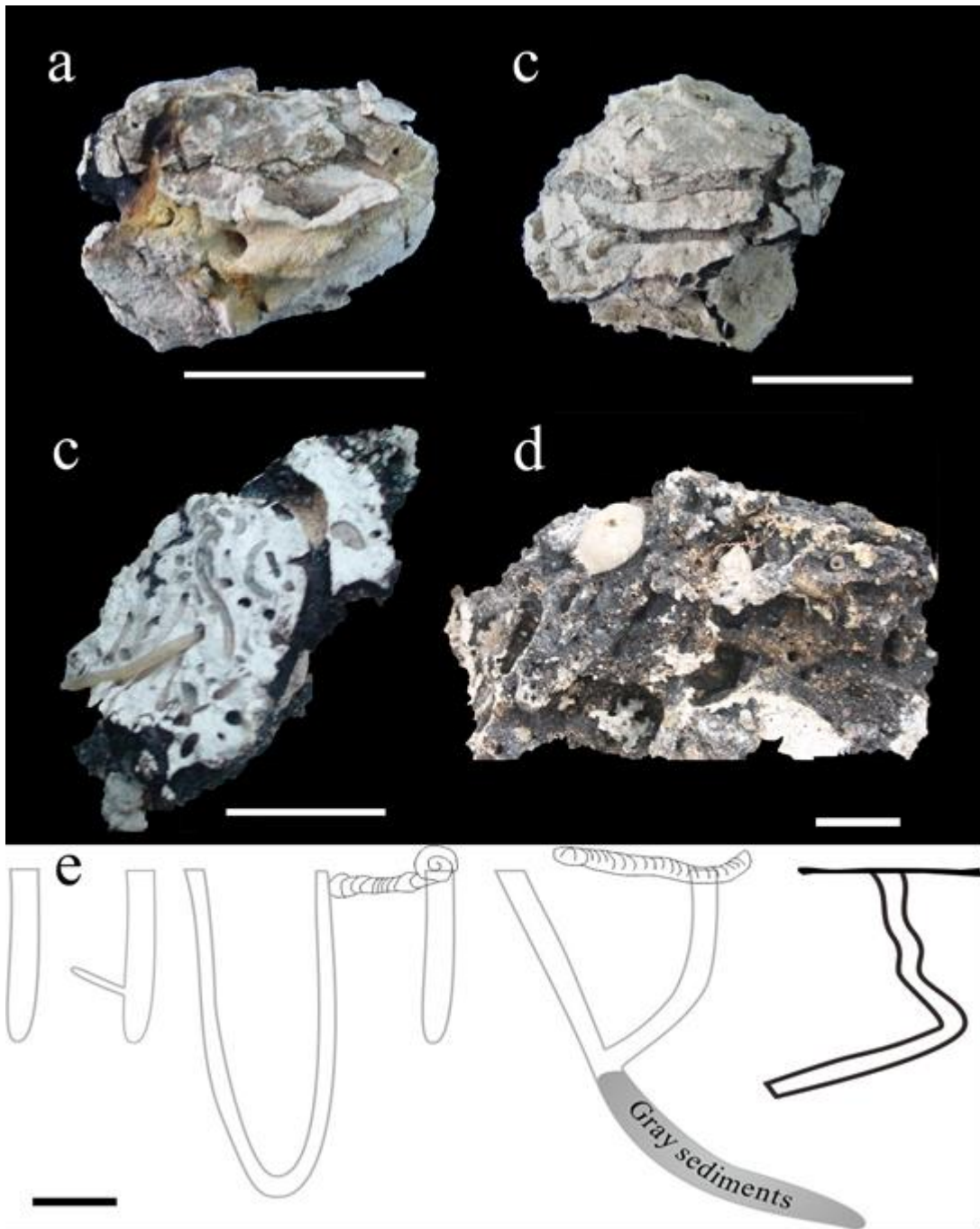
- Petrash, D. A., Lalonde, S. V., Gingras, M. K., and Konhauser, K. O.: A Surrogate approach to studying the chemical reactivity of burrow mucous linings in marine sediments, *Palaios*, 26, 594-600, <https://doi.org/10.2110/palo.2010.p10-140r>, 2011.
- Pimm, A., Garrison, R., and Boyce, R.: Sedimentology synthesis: lithology, chemistry and physical properties of sediments in the northwestern Pacific Ocean, in: *Initial Reports of the Deep Sea Drilling Project*, edited by: Fischer, A., and Heezen, B., U.S. Government Printing Office, Washington, 1131-1252, 1971.
- Plank, T., and Langmuir, C. H.: The chemical composition of subducting sediment and its consequences for the crust and mantle, *Chemical Geology*, 145, 325-394, [https://doi.org/10.1016/S0009-2541\(97\)00150-2](https://doi.org/10.1016/S0009-2541(97)00150-2), 1998.
- Qing, H., and Veizer, J.: Oxygen and carbon isotopic composition of Ordovician brachiopods: Implications for coeval seawater, *Geochimica et Cosmochimica Acta*, 58, 4429-4442, [https://doi.org/10.1016/0016-7037\(94\)90345-X](https://doi.org/10.1016/0016-7037(94)90345-X), 1994.
- Rae, J. W. B., Foster, G. L., Schmidt, D. N., and Elliott, T.: Boron isotopes and B/Ca in benthic foraminifera: proxies for the deep ocean carbonate system, *Earth and Planetary Science Letters*, 302, 403-413, <https://doi.org/10.1016/j.epsl.2010.12.034>, 2011.
- Raghukumar, C., Bharathi, P. A. L., Ansari, Z. A., Nair, S., Ingole, B. S., Sheelu, G., Mohandass, C., Nath, B. N., and Rodrigues, N.: Bacterial standing stock, meiofauna and sediment-nutrient characteristics: Indicators of benthic disturbance in the Central Indian Basin, *Deep-sea Research Part II-topical Studies in Oceanography*, 48, 3381-3399, [https://doi.org/10.1016/S0967-0645\(01\)00047-9](https://doi.org/10.1016/S0967-0645(01)00047-9), 2001.
- Rai, A. K., and Singh, V. B.: Late Neogene deep-sea benthic foraminifera at ODP Site 762B, eastern Indian Ocean: diversity trends and palaeoceanography, *Palaeogeography, Palaeoclimatology, Palaeoecology*, 173, 1-8, [https://doi.org/10.1016/S0031-0182\(01\)00299-1](https://doi.org/10.1016/S0031-0182(01)00299-1), 2001.
- Schlanger, S. O., and Douglas, R. G.: The Pelagic Ooze-Chalk-Limestone Transition and its Implications for Marine Stratigraphy, in: *Pelagic Sediments: On Land and under the Sea*, Blackwell Publishing Ltd., 117-148, 1974.
- Schmoker, J. W., and Halley, R. B.: Carbonate Porosity Versus Depth: A Predictable Relation for South Florida, *AAPG Bulletin*, 66, 2561-2570, 1982.
- Singh, R. K., Gupta, A. K., and Das, M.: Paleoceanographic significance of deep-sea benthic foraminiferal species diversity at southeastern Indian Ocean Hole 752A during the Neogene, *Palaeogeography, Palaeoclimatology, Palaeoecology*, 361-362, 94-103, <https://doi.org/10.1016/j.palaeo.2012.08.008>, 2012.
- Thompson, G., Bowen, V., Melson, W., and Cifelli, R.: Lithified carbonates from the deep-sea of the equatorial Atlantic, *Journal of Sedimentary Research*, 38, 1305-1312 1968.
- Wolfe, M. J.: Lithification of a carbonate mud: Senonian chalk in Northern Ireland, *Sedimentary Geology*, 2, 263-290, 1968.
- Xiong, Zhifang, Li, Tiegang, Algeo, Thomas, Chang, Fengming, Yin, and Xuebo: Rare earth element geochemistry of laminated diatom mats from tropical West Pacific: Evidence for more reducing bottomwaters and higher primary productivity during the Last Glacial Maximum, *Chemical Geology*, s 296-297, 103-118, <https://doi.org/10.1016/j.chemgeo.2011.12.012>, 2012.

Yu, J., Anderson, R. F., and Rohling, E. J.: Deep ocean carbonate chemistry and glacial-interglacial atmospheric CO₂ changes, *Oceanography*, 27, 16-25, 2014.



5

Figure 1: (a) Location of study area on the Southwest Indian Ridge. (b) Bathymetric map of area which show the location of the carbonate rock area (green ellipse), the active hydrothermal field (red circle), and the inactive hydrothermal field (red triangle).



5 Figure 2: Deep-sea carbonate rocks collected from the SWIR. (a) A carbonate rock sample shows empty burrows are partly covered by ferromanganese crusts. (b) Straight and branched burrows are infilled by grey sediments. (c) Abundant burrows, as well as a benthic fauna (polychaete worm), are present on a cross section of a carbonate rock. (d) An echinoid, together with other benthic faunas, burrows on a carbonate rock with the honeycombed structures and encrusted by thin ferromanganese crusts. (e) Sketch for different burrow structures in deep-sea carbonate rocks collected from the SWIR. Scale bar of a, c are 5cm, and the b, d e is 3 cm.

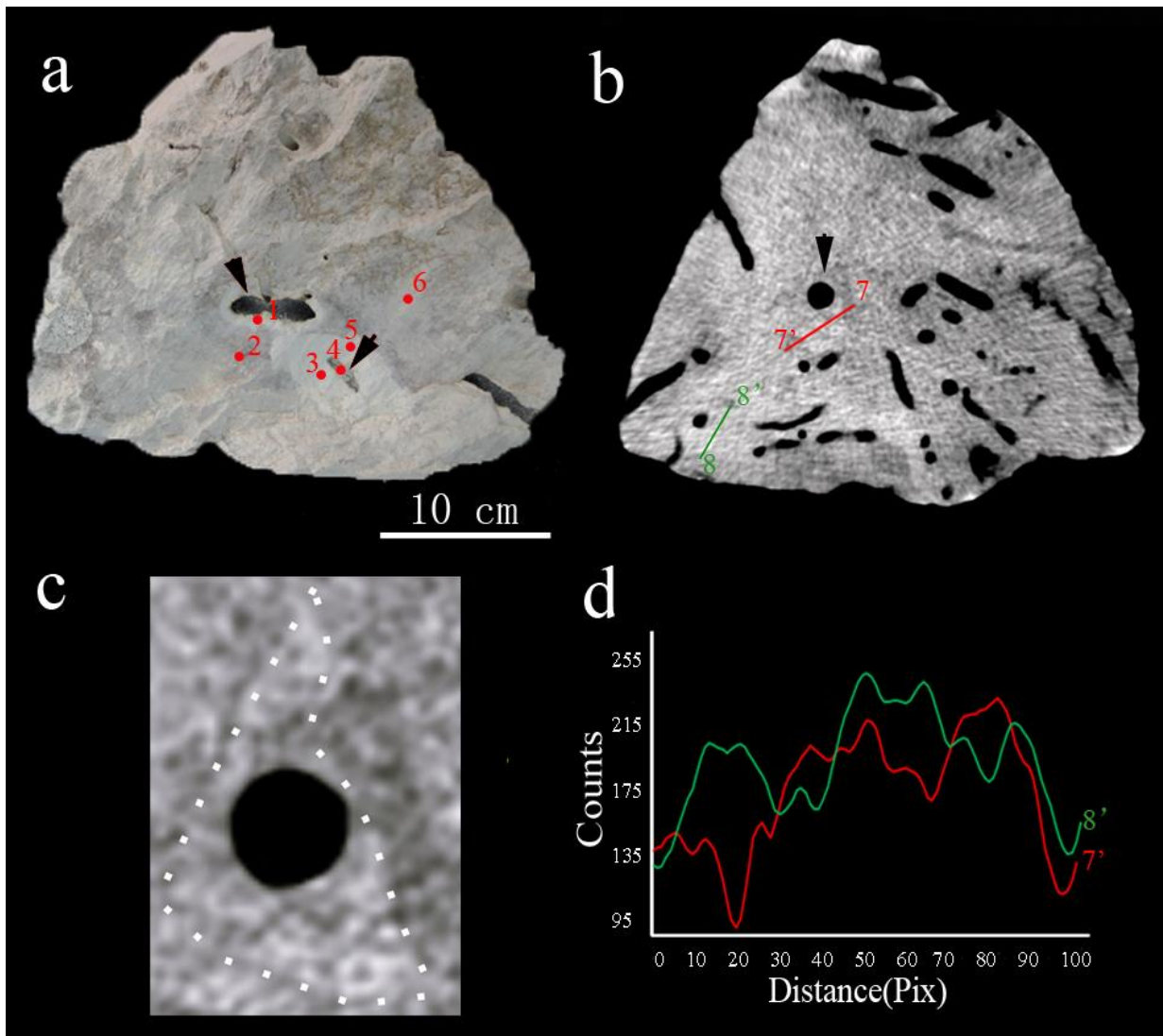


Figure 3: (a) A hand specimen shows the enhancement of brightness associated with burrow structures. Numbers of red dots indicate the subsamples for carbon and oxygen isotope analysis in table 1. (b) Tomographic cross-section of the sample reveals that abundant burrows are clearly present in the interior of the samples. Higher density areas with triangular, hexagonal and irregular shapes. (c) The enlargement of Figure 3b shows the triangular shape of higher density (white dash line). (d) Line scan profiles of gray values along solid line (7-7' and 8-8') in Figure 3b.

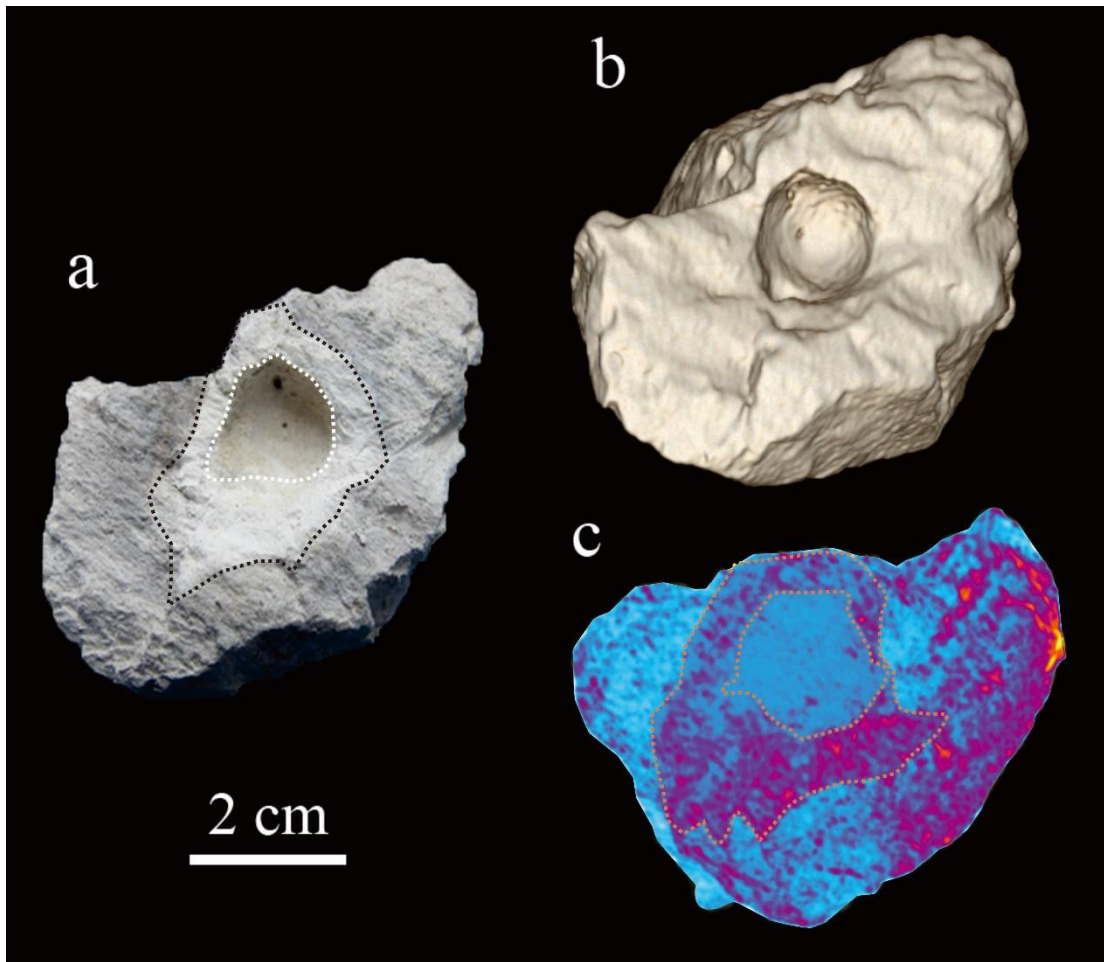


Figure 4 (a) A carbonate rock sample shows the enhancement of brightness associated with a burrow structure. (b) 3D reconstruction of the sample by CT shows the morphology of the sample. (c) 3D reconstruction of the sample by CT exhibits that the enhancement of density is visible around the burrow, which is consistent with the enhancement of brightness around the burrow as shown in Fig.4 a.

5

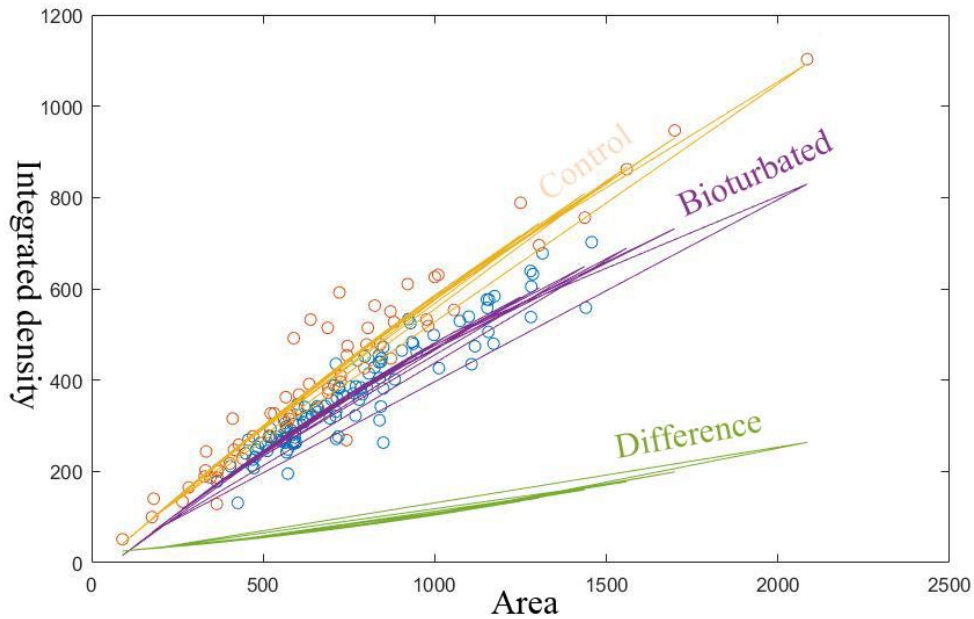
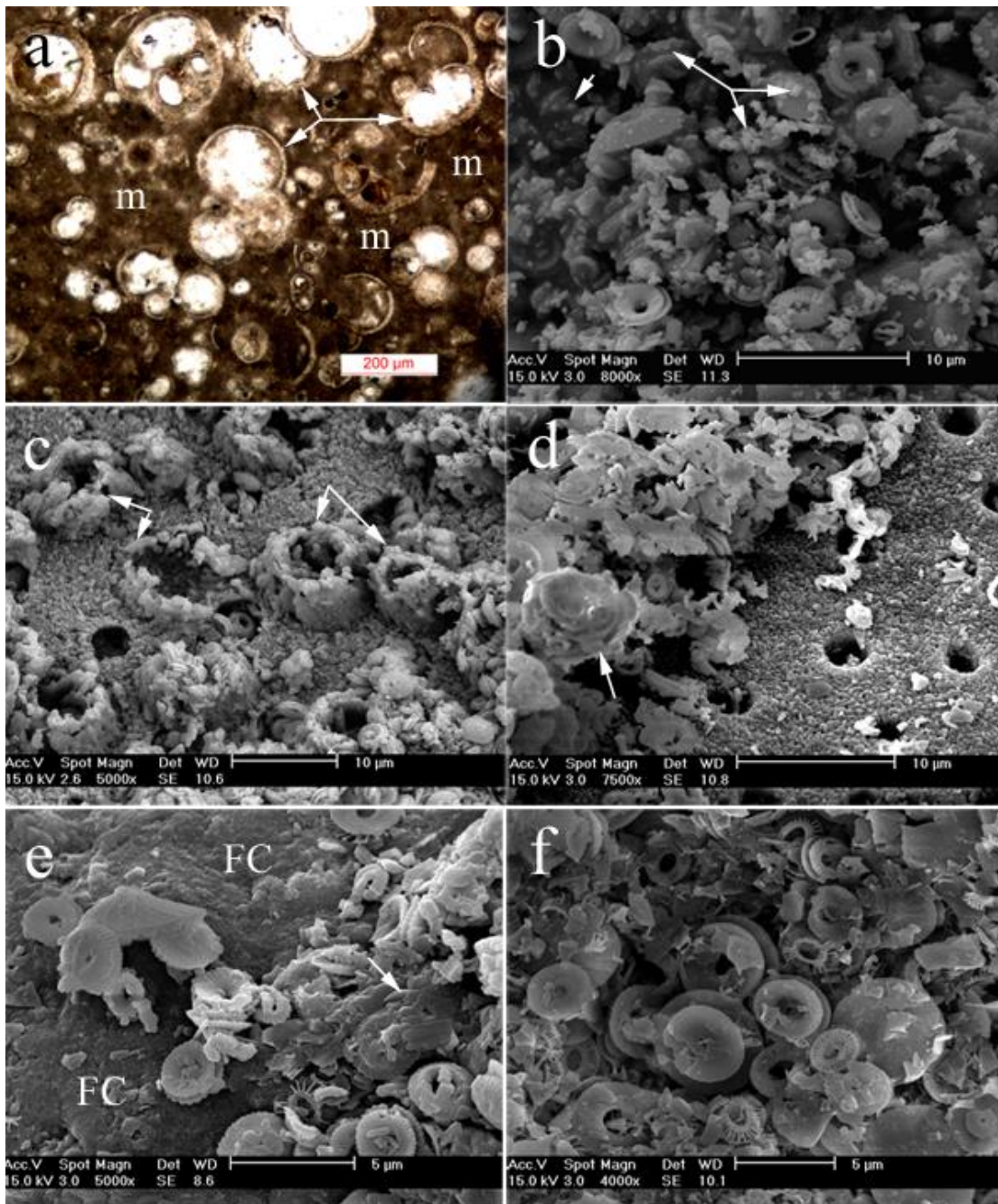
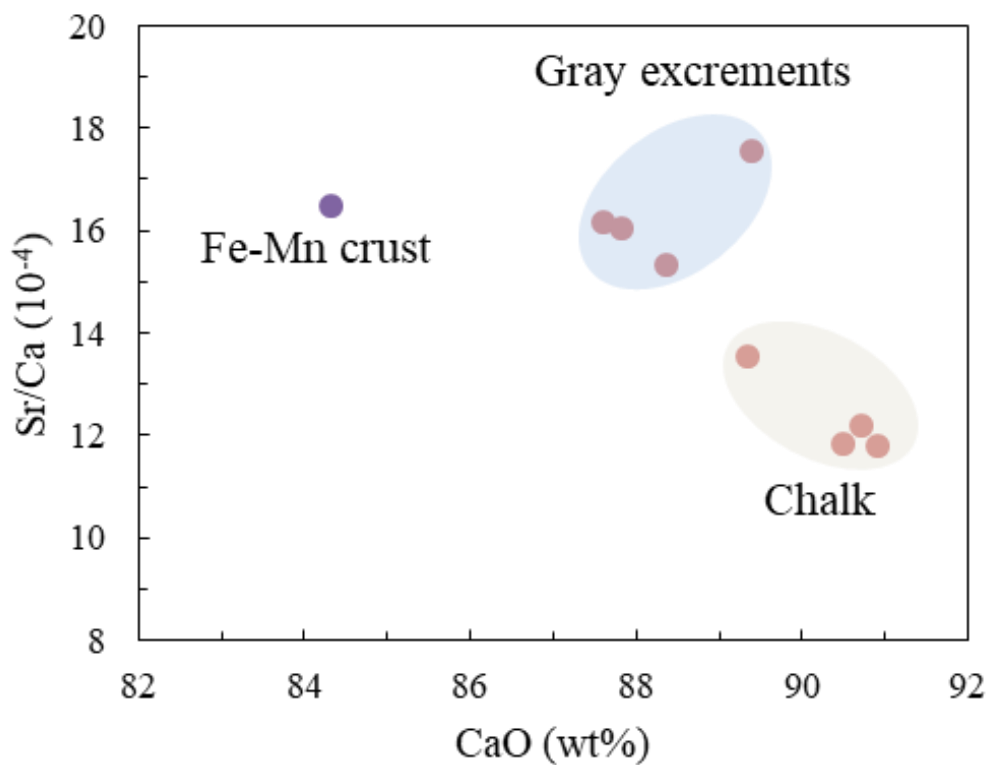


Figure 5 Statistical analysis of integrated density extracted from selected area around burrow and paralleled undisturbed area clearly shows different density around the burrows. Both images were inverted so that bigger integrated density means a darker colour in original CT image. The total number of analyzed burrows are 113. With 95% confidence bounds, the goodness of fit is showed by $R^2_{\text{bioturbate}}=0.9312$ and $R^2_{\text{control}}=0.8802$.



the dissolution of the coccoliths. (f) Scanning electron micrograph shows grey sediments which infill the burrow. Smooth surfaces of the coccoliths indicate that the dissolution commonly occurs.



5 Figure 7: The lower of Sr/Ca in chalk compared to the gray excrements represents the lithification of different portions of carbonate.

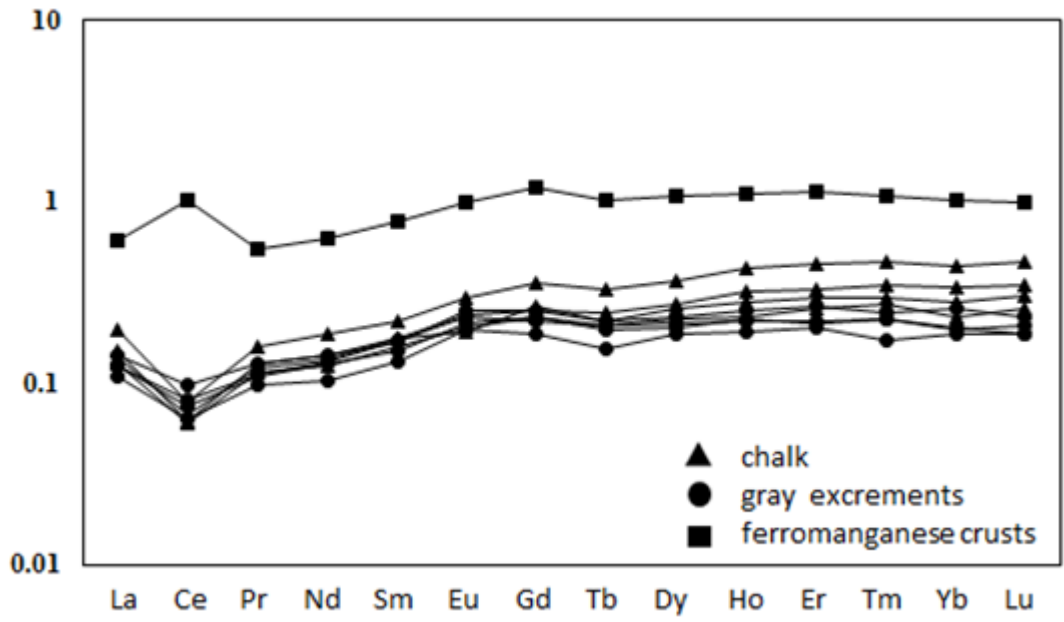


Figure 8: PAAS-normalized REE distribution patterns of selected samples from the SWIR.

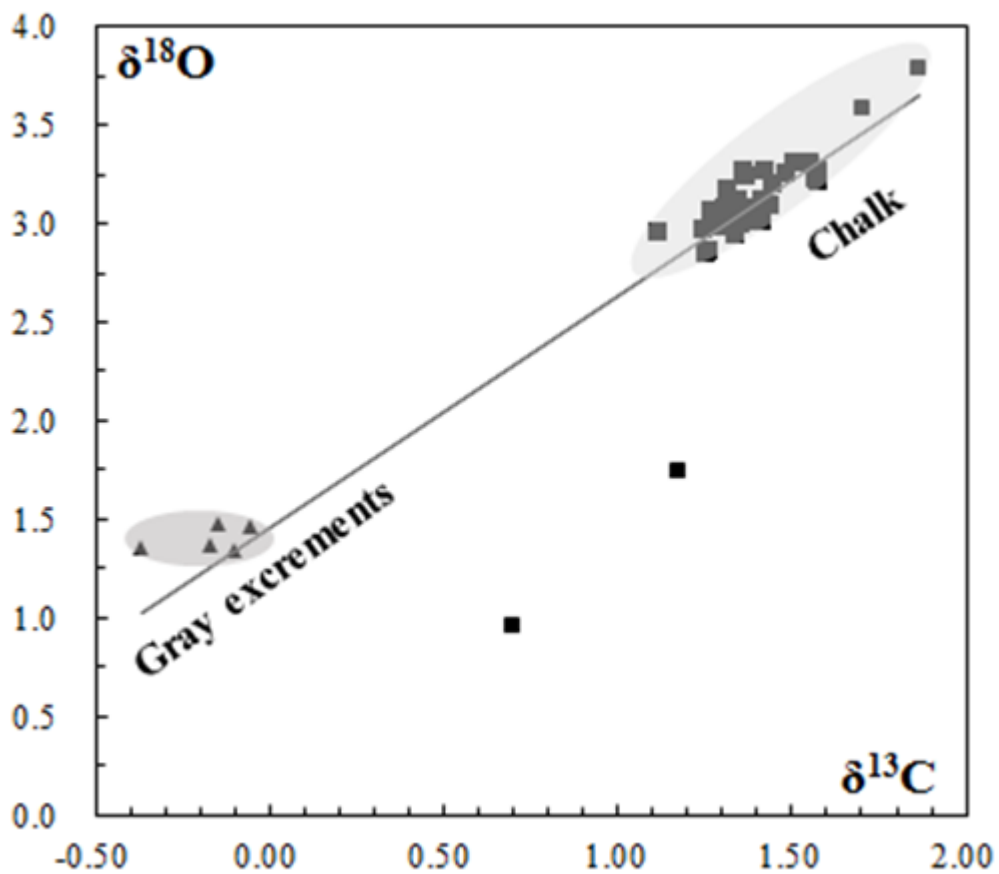


Figure 9 Oxygen and carbon isotopic composition of carbonate samples from the SWIR. Gray excrements contain the light carbon and oxygen isotopic values compared to the chalk. The $\delta^{13}\text{C}_{\text{PDB}}$ values of chalk and gray excrements are positively correlated with $\delta^{18}\text{O}_{\text{PDB}}$ values ($r=0.91$).

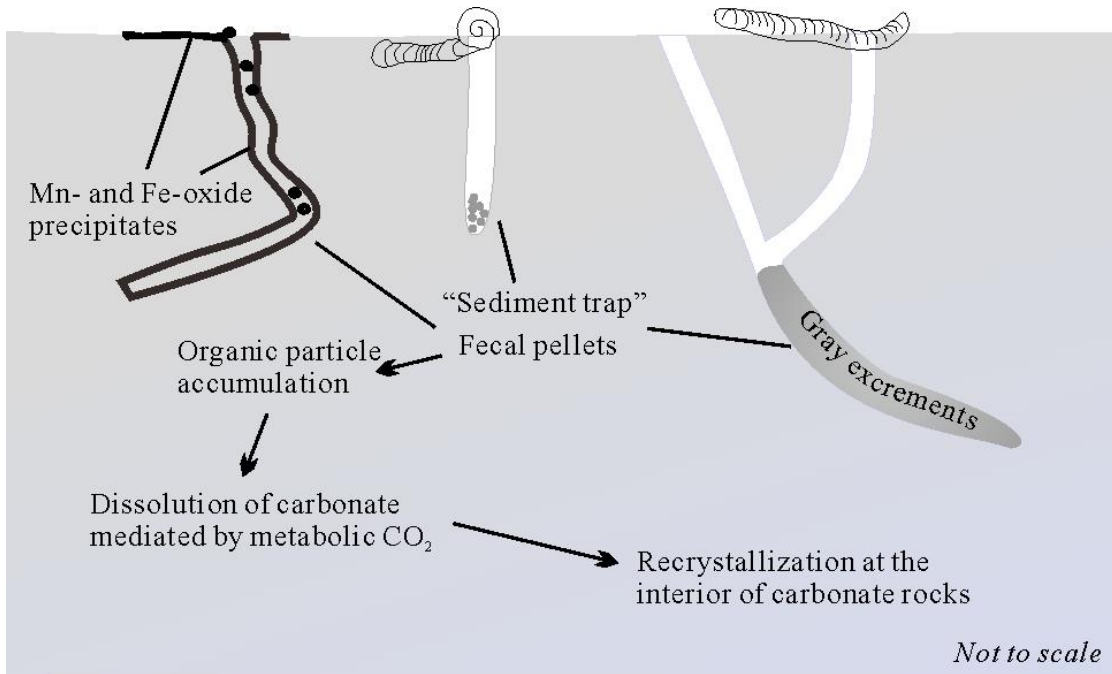


Figure 10 Schematic model for carbonate lithification influenced by bioturbation on the SWIR.

5

Sample NO.	$\delta^{13}\text{C PDB}$	$\delta^{18}\text{O PDB}$
1	1.36	3.04
2	1.28	2.99
3	1.30	3.09
4	-0.37	1.56
5	1.28	3.00
6	1.11	2.97

10

Table 1 Isotope data for samples collected from the Figure 3a. 1, 3 and 5 represent the higher density influenced by bioturbation compared to 2 and 6. 4 represents gray excrements infilled in the burrows.

15